AMERICAN SOCIETY FOR MICROBIOLOGY | Journal of Virology®

VIRUS-CELL INTERACTIONS

Identification of H209 as Essential for pH 8-Triggered Receptor-Independent Syncytium Formation by S Protein of Mouse Hepatitis Virus A59

Pei Li,[a] Yiwei Shan,[a] Wangliang Zheng,[a] Xiuyuan Ou,[a] Dan Mi,[a] Zhixia Mu,[a] Kathryn V. Holmes,[b] Zhaohui Qian[a]

[a]MOH Key Laboratory of Systems Biology of Pathogens, Institute of Pathogen Biology, Chinese Academy of Medical Sciences and Peking Union Medical College, Beijing, China

[b]Department of Microbiology, University of Colorado School of Medicine, Aurora, Colorado, USA

ABSTRACT The spike glycoprotein (S) of murine coronavirus mouse hepatitis virus (MHV) strain A59 uses murine carcinoembryonic antigen-related cell adhesion molecule 1a as its receptor for cell entry, but S protein can also be triggered in the absence of receptor by pH 8.0 alone at 37°C. The mechanism by which conformational changes of this S glycoprotein can be triggered by pH 8.0 has not yet been determined. Here, we show that MHV-A59 S protein is triggered by pH 8.0 at 37°C to induce receptor-independent syncytium (RIS) formation on 293T cells, and that the conformational changes in S proteins triggered by pH 8.0 are very similar to those triggered by receptor binding. We systemically mutated each of 15 histidine residues in S protein and found that H209 is essential for pH 8.0-triggered RIS formation, while H179, H441, H643, and H759 also play important roles in this process. Replacement of H209 with Ala had no effect on receptor binding, but in murine 17Cl.1 cells mutant H209A MHV-A59 showed delayed growth kinetics and was readily outcompeted by wild-type virus when mixed together, indicating that the H209A mutation caused a defect in virus fitness. Finally, the H209A mutation significantly increased the thermostability of S protein in its prefusion conformation, which may raise the energy barrier for conformational change of S protein required for membrane fusion and lead to a decrease in virus fitness in cell culture. Thus, MHV-A59 may have evolved to lower the stability of its S protein in order to increase virus fitness.

IMPORTANCE Enveloped viruses enter cells through fusion of viral and cellular membranes, and the process is mediated by interactions between viral envelope proteins and their host receptors. In the prefusion conformation, viral envelope proteins are metastable, and activation to the fusion conformation is tightly regulated, since premature activation would lead to loss of viral infectivity. The stability of viral envelope proteins greatly influences their activation and virus fitness. Here, we report that, similar to the A82V mutation in Ebola glycoprotein, in the S glycoprotein of murine coronavirus MHV-A59, the histidine residue at position of 209 significantly affects the thermal stability of the S protein, determines whether S protein can be activated at 37°C by either pH 8.0 alone or by receptor binding, and affects viral fitness in cell culture. Thus, the spike glycoprotein of MHV-A59 has evolved to retain histidine at position 209 to optimize virus fitness.

KEYWORDS mouse hepatitis virus, coronavirus spike glycoprotein, coronavirus receptor-independent syncytium formation, coronavirus S glycoprotein thermal stability, S protein conformational change

Enveloped viruses enter cells through fusion of viral and host cellular membranes, and they employ diverse molecular mechanisms to mediate membrane fusion. Although binding to receptors on host cells by viral envelope glycoproteins (Gp) is

Received 6 February 2018 **Accepted** 5 March 2018

Accepted manuscript posted online 7 March 2018

Citation Li P, Shan Y, Zheng W, Ou X, Mi D, Mu Z, Holmes KV, Qian Z. 2018. Identification of H209 as essential for pH 8-triggered receptor-independent syncytium formation by S protein of mouse hepatitis virus A59. J Virol 92:e00209-18. https://doi.org/10.1128/JVI.00209-18.

Editor Tom Gallagher, Loyola University Medical Center

Address correspondence to Zhaohui Qian, zqian2013@sina.com.

P.L. and Y.S. contributed equally to this study.

clearly a prerequisite for virus entry, some enveloped viruses, like influenza and vesicular stomatitis viruses (VSV) (1, 2), also require low pH to activate the membrane fusion activity of their viral glycoproteins, whereas other enveloped viruses, like respiratory syncytial virus (RSV) and human immunodeficiency virus (HIV) (3, 4), can enter cells at the plasma membrane and acidic pH is not required for virus entry.

Coronaviruses (CoVs) are enveloped viruses with single-stranded plus-sense RNA genomes ranging in size from 26 to 32 kb. Coronaviruses are phylogenetically divided into four genera, alphacoronaviruses (α-CoV), betacoronaviruses (β-CoV), gammacoronaviruses (γ-CoV), and deltacoronaviruses (δ-CoV) (5, 6). Mouse hepatitis viruses (MHV) are a group of murine β-CoVs in lineage A that have been widely utilized as models for studying coronaviral pathogenesis. The two most commonly studied strains of MHV are MHV-A59 and MHV-JHM. The entry of MHV is mediated by the interaction between the trimeric ~180-kDa viral spike (S) protein and its cellular receptor, murine carcinoembryonic antigen-related cell adhesion molecule 1a (mCEACAM1a) (7). This coronavirus S protein is a class I viral fusion protein. During virus maturation, S glycoproteins of most strains of MHVs are cleaved in the Golgi by furin-like enzymes to form the ~90-kDa S1 and S2 subunits (8, 9). S1 contains the receptor binding domain (RBD) (10, 11), and S2 contains the membrane fusion machinery (8). Cleavage between S1 and S2 is critical for S protein-mediated cell-cell fusion (also called syncytium formation) (9), and additional cleavage(s) of S2 is required for virus entry (12–14) and is thought to release the restraint of the fusion peptide of the S2 subunit to allow it to insert into its target cell membrane (15, 16).

The effect of pH on receptor-dependent entry of MHV is still unclear. Some early studies showed that infection of murine cells with MHV-A59 caused extensive cell-cell fusion at neutral pH, indicating that MHV-A59 enters cells through a pH-independent pathway (17–20), while other studies observed a reduction in infection of MHV-A59 after cells were treated with lysosomotropic agents, suggesting that low pH facilitates the entry of MHV-A59 (16, 21, 22). Unlike the controversial role of low pH in receptor-dependent MHV-A59 virus entry, alkaline pH alone has a marked effect on conformational changes of MHV-A59 S protein in a receptor-independent manner (18, 19). Incubation of MHV-A59 virus at 37°C and pH 8.0 without receptor significantly decreases virus infectivity and triggers S protein to form a conformation similar to that induced by receptor binding (19, 23). In this study, we identified H209 as the major sensor for pH 8-triggered, receptor-independent conformational change of S protein, leading to syncytium formation, and showed that the H209A mutant MHV-A59 was defective in both virus growth kinetics and fitness.

RESULTS

High pH-triggered and receptor-independent syncytium formation by MHV-A59 S protein. Although human 293T cells are not susceptible to infection with MHV-A59 virus (data not shown) or lentivirus pseudotyped with MHV-A59 S protein (Fig. 1A), large syncytia were formed when the cells were transfected with the plasmid encoding codon-optimized MHV-A59 S glycoprotein and cultured with medium at pH 7.0 or above (green fluorescent protein [GFP]-expressing plasmids were cotransfected into the cells to make syncytia easier to visualize) (Fig. 1B). The average size of syncytia in 293T cells and the percentage of nuclei in syncytia increased as pH increased (Fig. 1B), indicating that receptor-independent fusion mediated by MHV-A59 S protein is alkaline pH dependent, in agreement with previous reports (18, 19).

Conformational changes of MHV-A59 S protein triggered by pH 8.0 are similar to those triggered by receptor binding. We next determined if the elevated pH-triggered, receptor-independent conformational changes of MHV-A59 S proteins were similar to conformational changes induced by receptor binding. Purified lentivirus pseudovirions with MHV-A59 S proteins were incubated under the indicated conditions and treated with limited trypsin digestion. Consistent with our previous report (15), the majority of native S proteins in pseudovirions (Fig. 1C, lane 14) were cleaved into S1 and S2, and both migrated around 90 kDa when the boiled and dithiothreitol (DTT)-treated

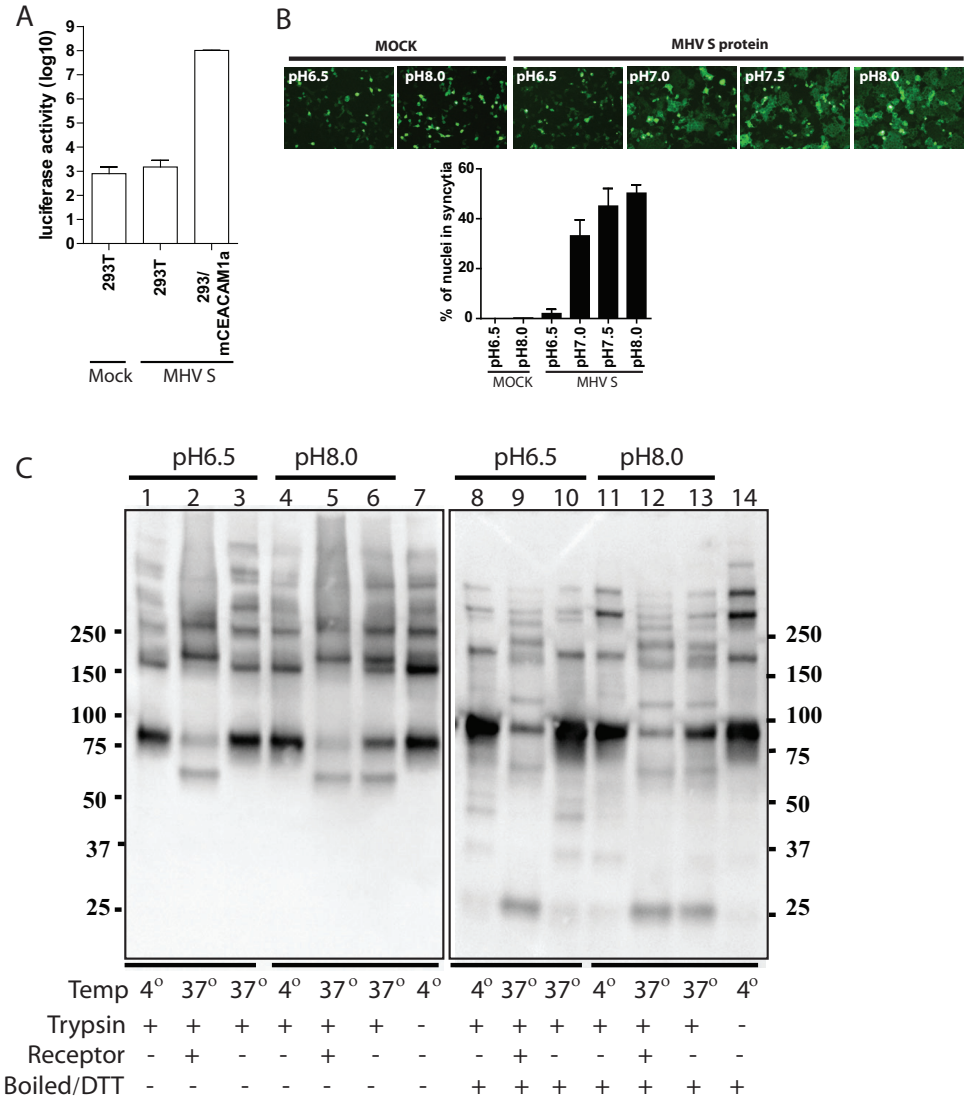

FIG 1 Receptor-independent syncytium (RIS) formation and conformational changes in MHV-A59 S glycoprotein triggered by elevated pH. (A) HEK293T cells are not susceptible to transduction by MHV S protein pseudovirion. The transduction was measured according to luciferase activities. The experiments have been done three times in triplicate, and one representative is shown as means with standard deviations. (B) Elevated pH-induced receptor-independent syncytium formation in HEK293T cells. HEK293T cells expressing MHV S protein and GFP were incubated at the indicated pHs for 3 h. (Top) Representative images. (Bottom) Quantitative analysis of syncytia. Data shown are representative of three independent experiments. (C) Limited trypsin digestion of S protein of MHV-A59. Lentivirus pseudovirions with MHV-A59 S protein were incubated under the indicated conditions for 30 min and then digested on ice with 20 μg/ml trypsin for 20 min. S proteins and fragments were detected using goat anti-MHV S antibody AO4. Experiments were performed either without boiling and no DTT (left) or with boiling and DTT (right). The experiments were repeated twice, and one representative is shown.

proteins were separated in SDS-PAGE and detected with polyclonal goat anti-MHV-A59 S AO4 antibodies. A weaker band around 180 kDa reflects uncleaved S protein. The bands above 180 kDa may reflect dimers and trimers of S proteins on the pseudovirions. When the pseudovirions were incubated at 4°C in the absence of the receptor, limited trypsin digestion did not significantly alter the pattern of Western blot results (lanes 1, 4, 8, and 11) compared to the no-trypsin control (lanes 7 and 14), and there was no marked difference between different pH treatments at 4°C. In contrast, at 37°C, pH 8.0 had significant effects on the conformational changes of S protein in the absence of the receptor (lanes 6 and 13), while pH 6.5 showed minimal effects (lanes 3 and 10) compared to the no-trypsin control. Upon limited trypsin digestion, several

new bands were generated in MHV-A59 S proteins on pseudovirions that were incubated at 37°C and pH 8.0. There was a new ~60-kDa band in the sample without boiling and DTT treatment (lane 6) and multiple bands, including 25 kDa, 65 kDa, 120 kDa, etc., in the boiled and DTT-treated sample (lane 13). The overall pattern of pH 8.0-triggered receptor-independent conformational changes of MHV-A59 S protein at 37°C was very similar to what happened when MHV-A59 S proteins were incubated with the soluble receptor mCEACAM1a[1-4] at 37°C (lanes 2, 5, 9, and 12). Consistent with previous reports (18, 19), pH seems to have no effect on receptor-induced conformational changes of MHV-A59 S proteins (lanes 2, 5, 9, and 12).

Identification of H209 as essential for pH 8.0-triggered receptor-independent syncytium formation. Histidine (His) is the only amino acid residue with a side chain that has a pK_a close to physiological pH, allowing it to serve as either an acid or as a base depending on local pH conditions (24). Histidine plays essential roles in pH sensing and conformational changes of the envelope glycoproteins of several other viruses (25–28). Moreover, histidine has been shown to be critical for pH-dependent S protein-mediated cell fusion in OBL60 virus (29), an MHV-4 variant. There are 15 histidine residues in the ectodomain of the MHV-A59 S protein (Fig. 2A). We asked whether any of them is responsible for pH-triggered, receptor-independent conformational changes of MHV-A59 S protein. Individual alanine (Ala) substitutions were introduced separately into each of these His positions. We first determined if any of the Ala mutations affected glycoprotein expression and processing in human 293T cells. Similar to what was observed in MHV-A59 S protein on pseudotyped lentivirions, there was a major band around 90 kDa reflecting cleaved S proteins and a minor band around 180 kDa reflecting full-length S proteins detected in the cell lysate of 293T cells expressing wild-type (WT) MHV-A59 S protein (Fig. 2B). Compared to the WT, most of the Ala mutants had no effect on S protein expression and processing (Fig. 2B). However, the H205A, H463A, and H506A mutants markedly decreased the expression and processing of cleaved S proteins, while the H1098A and H1114A mutants almost abolished the expression and processing of cleaved S proteins (Fig. 2B). With two-thirds of the His/Ala mutants showing no effects on S protein expression and processing, we next investigated if any of these might affect transport of the S protein to the cell surface. Human 293T cells expressing WT or mutant S proteins were incubated on ice with goat polyclonal anti-MHV S protein antibody AO4 and analyzed by flow cytometry. All mutant S proteins showing WT levels of expression in the cell lysate also showed WT levels of S protein on the cell surface (Fig. 2C). We next determined whether any of these mutations influence the folding and conformation changes of MHV-A59 S proteins using a soluble receptor binding assay. Human 293T cells transiently expressing WT or His/Ala mutant S proteins were incubated with the soluble receptor mCEACAM1a[1-4] at 4°C, and their receptor binding affinity was measured using flow cytometry. All of the mutant MHV-A59 S proteins that showed WT levels of expression and processing in cells also bound to soluble mCEACAM1a[1-4] at levels similar to that of WT S protein (Fig. 2D), indicating that their conformations were similar to that of the WT.

To determine whether any of the Ala mutants affect high pH-triggered, receptor-independent cell fusion by MHV-A59 S protein, human 293T cells were transfected with plasmids encoding different Ala mutant MHV-A59 S proteins and then cultured in pH 8.0 medium to induce syncytium formation. While there were no syncytia observed in mock-transfected 293T cells, WT MHV-A59 S proteins induced large syncytia at pH 8.0 and 37°C, and syncytium formation was pH dependent, since there was only a low background level of syncytia observed when S protein-expressing cells were cultured in pH 6.5 medium. Among the Ala mutants showing WT levels of expression and conformation, at pH 8.0, the H428A, H523A, H538A, H716A, and H760A mutant S proteins induced large syncytia at levels similar to that of the WT (Fig. 3A and B), whereas the H209A mutant only gave background levels of syncytia. In addition, the H179A, H441A, H643A, and H759A mutants showed significantly smaller syncytia (Fig. 3A).

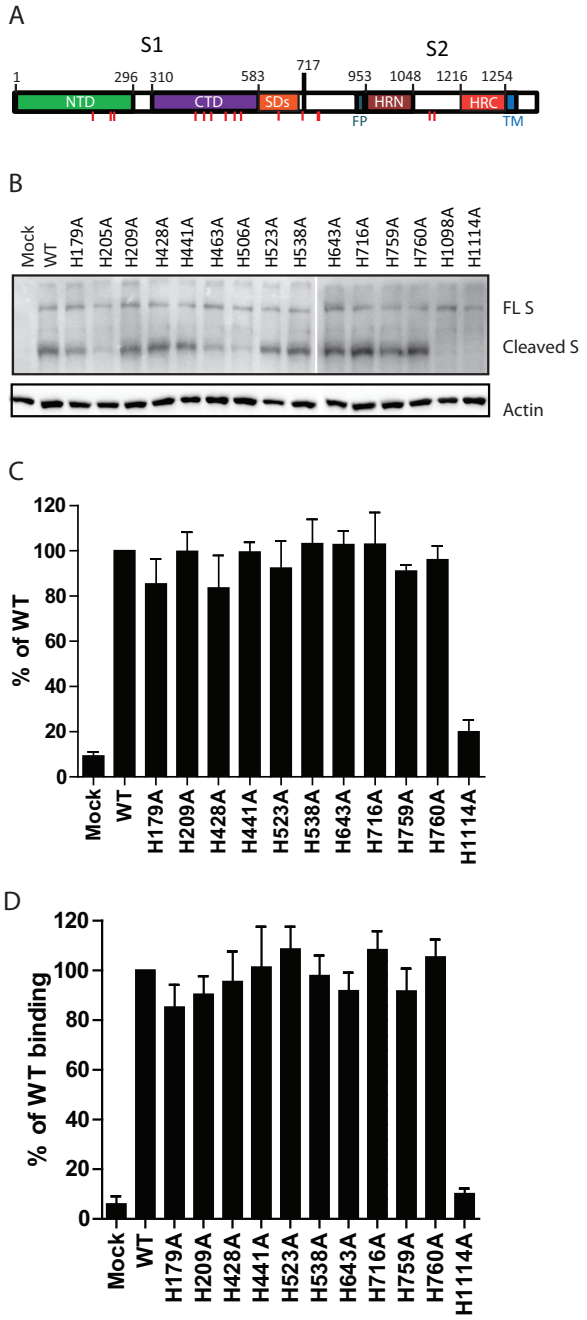

FIG 2 Analysis of expression and receptor binding activities of mutant MHV-A59 S proteins. (A) Schematic diagram of MHV S protein. NTD, N-terminal domain; CTD, C-terminal domain; SD, subdomains; FP, fusion peptide; HRN, N-terminal heptad repeat; HRC, C-terminal heptad repeat; TM, transmembrane domain. The location of each individual histidine is indicated by a short vertical red line. (B) Western blot analysis of expression of WT or mutant MHV S protein in cell lysate. The ~180-kDa full-length (FL) and ~90-kDa S1 and S2 subunits (cleaved S) of MHV-A59 S protein were detected by using goat anti-MHV S antibody AO4; β-actin was detected with mouse monoclonal anti-actin antibody. (C) Analysis of surface expression of mutant MHV-A59 S protein by flow cytometry. MHV-A59 S protein-expressing 293T cells were stained with polyclonal goat anti-MHV S antibody AO4. The amount of wild-type S protein on the cell surface was set to 100%. All of the experiments shown were repeated at least three times. Data are shown as means ± standard deviations. (D) Receptor binding activities of WT and Ala mutant S proteins. MHV S protein-expressing 293T cells were incubated with soluble receptor, AVI-tagged mCEACAM1a, followed by polyclonal rabbit anti-AVI antibody and fluorescein isothiocyanate-conjugated goat anti-rabbit IgG. The results from the wild type were set to 100%, and the experiments were repeated three times. Data are shown as means ± standard deviations.

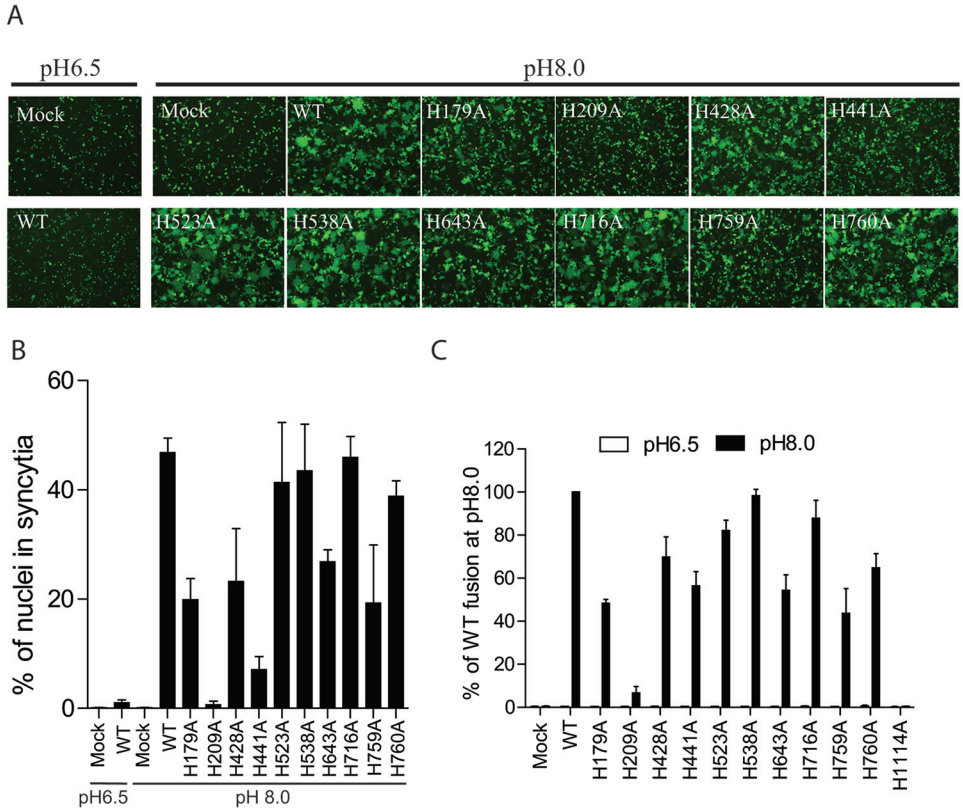

FIG 3 Receptor-independent syncytia mediated by WT or mutant MHV-A59 S protein. MHV S protein-expressing 293T cells were transiently transfected with eGFP and then incubated with medium at either pH 6.5 or 8.0 for 3 h. (A) Representative images; (B) percentage of nuclei in syncytia. The experiments were done at least three times, and means with standard deviations are shown. (C) Quantitative analysis of receptor-independent syncytia by measurement of luciferase activities. MHV S protein-expressing 293T cells transfected with pFR-Luc were incubated with 293T cells transfected with pBE-NF-κB for 6 h with medium at either pH 6.5 or 8.0. The experiments were done at least three times, and means with standard deviations are shown.

We also quantified the effects of individual Ala mutations on receptor-independent syncytium formation (RIS) using the modified quantitative fusion assay that we previously developed (15). Human 293T cells transiently transfected with pBD-NF-κB plasmid were overlaid onto the human 293T cells transiently cotransfected with pFR-Luc plasmid and plasmid encoding either WT or mutant MHV-A59 S protein. The plasmid pBD-NF-κB encodes a fusion protein with the DNA binding domain of GAL4 and the transcription activation domain of NF-κB, and pFR-Luc contains a synthetic promoter with five tandem repeats of the yeast GAL4 binding sites controlling the expression of the luciferase gene. Once the two types of cells fuse, binding of GAL4-NF-κB fusion protein to GAL4 promoter drives the expression of luciferase, and the relative fusion activities of the WT and mutant proteins can thus be determined. Compared to mock-transfected and pH 6.5 controls, incubation of WT S protein-expressing cells with pBD-NF-κB cells at pH 8.0 resulted in about a 300-fold increase in luciferase activity. Overall, the pattern of effect of individual Ala mutations on alkaline pH-triggered, receptor-independent cell-cell fusion measured by this quantitative method (Fig. 3C) was very similar to that of the nonquantitative method (Fig. 3A and B). All mutant S proteins (H179A, H428A, H441A, H523A, H538A, H643A, H716A, H759A, and H760A) that showed WT levels of expression and processing of S protein also induced receptor-independent cell-cell fusion at pH 8.0 at levels of greater than or equal to 40% of the WT, except for H209A. At pH 8.0 the H209A mutant had only about 6% of the cell fusion activity of WT S protein, indicating that H209 plays an essential role in elevated pH-triggered RIS mediated by MHV-A59 S proteins.

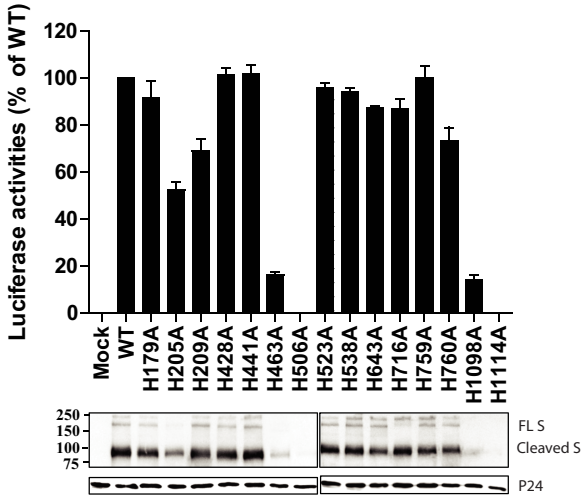

FIG 4 Receptor-dependent entry of lentivirus pseudovirions with wild-type or Ala mutant S proteins of MHV-A59 on HeLa/mCEACAM1a cells. (Top) Pseudovirus entry was quantitated by luciferase activity at 40 h postinoculation. A typical transduction by wild-type S protein pseudoviruses resulted in an increase of luciferase activity of over 10,000-fold. The experiments were repeated at least three times, and averages from three experiments with standard deviations are shown. (Bottom) Detection by Western blot analysis of wild-type or mutant S proteins incorporated into pseudovirions. S proteins were detected using goat anti-MHV S antibody AO4; p24, a gag protein of HIV, was detected using rabbit anti-p24 antibodies. FL S, full-length S protein. The experiments were repeated at least three times.

H209A mutation had minor effect on transduction efficiency by MHV-S pseudovirions. To determine whether any of the Ala mutations influenced receptor-dependent coronavirus entry, HeLa cells stably expressing mCEACAM1a (HeLa/mCEACAM1a) were transduced with lentiviruses pseudotyped with either WT or mutant MHV-A59 S proteins. Consistent with our previous reports (15), transduction of HeLa/mCEACAM1a cells with WT lentiviruses pseudotyped with MHV-A59 S protein resulted in a more than 10,000-fold increase of luciferase activity compared to that of the mock control (Fig. 4). While H179A, H428A, H441A, H523A, H538A, H643A, H716A, H759A, and H760A gave WT levels of transduction, H209A and H760A consistently reduced the level of transduction by about 30% (Fig. 4), even though these mutant S proteins were incorporated into pseudovirions as efficiently as the WT (Fig. 4) and bound to the receptor as well as the WT (Fig. 2C). Mutants H205A, H463A, H506A, H1098A, and H1114A likely caused reduced transduction because their S proteins were poorly incorporated into pseudovirions.

H209A mutant MHV-A59 is attenuated in cell culture. Since the H209A mutation almost abolished pH 8.0-triggered receptor-independent fusion by MHV-A59 S proteins and also slightly decreased receptor-dependent transduction efficiency by pseudovirions with MHV-A59 S protein, we next investigated what would happen when H209A was introduced into MHV-A59 virions. Using targeted RNA recombination (TRR), the H209A mutation was introduced into the MHV-A59 viral genome, the recombinant virus was propagated in murine 17Cl.1 cells, and the mutation in the viral genome was verified by nucleotide sequencing. As shown in Fig. 5A, H209A mutation had minimal effect on S protein expression and incorporation into MHV. However, when murine 17Cl.1 cells were inoculated with WT or H209A virus at a multiplicity of infection (MOI) of 0.05, there were marked differences in their syncytium formation activity. The timing of syncytium formation induced by infection of H209A virus was significantly delayed compared to that of WT virus (Fig. 5B). At 8 and 12 h postinoculation, release of H209A virus from the cells was 25-fold and 22-fold less than that for the WT virus, respectively (Fig. 5C), indicating that H209A mutant virus growth and/or release was significantly delayed. Interestingly, by 24 h postinoculation, the yield of H209A virus released was almost the same as that of the WT, and by 36 and 48 h postinoculation the yield of H209A virus was significantly greater than that of WT virus, probably because the

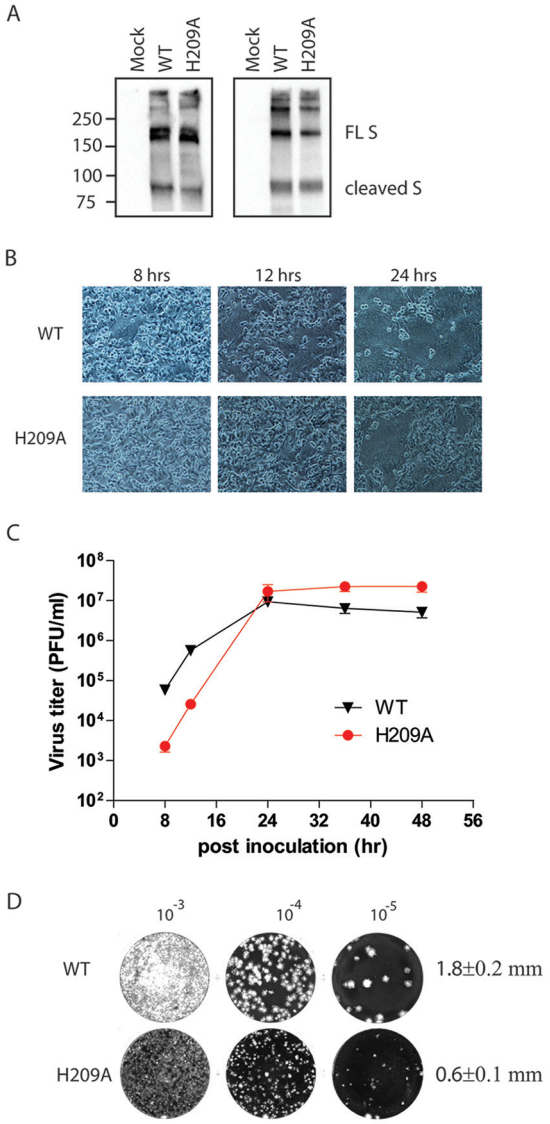

FIG 5 Infection of murine 17 Cl.1 cells by WT or H209A mutant MHV-A59 virus. (A) Western blot analysis of WT or mutant S protein expression and incorporation in MHV. The 17Cl.1 cells were inoculated with either the WT or H209A mutant virus at an MOI of 0.05. The S proteins were detected using polyclonal goat anti-MHV-S antibody AO4 at 24 h postinoculation. (Left) Cell lysate; (right) MHV virions. (B) Syncytium formation. The 17Cl.1 cells were inoculated with the indicated viruses at an MOI of 0.05, and the representative pictures were taken at 8, 12, and 24 h postinoculation. (C) Virus growth. WT or mutant viruses were inoculated on 17Cl.1 cells at an MOI of 0.05; virus-containing supernatant media were harvested at 8, 12, 24, 36, and 48 h postinoculation and titrated on 17Cl.1 cells using plaque assay. Data are shown as means with standard deviations. (D) Plaque morphology of WT and H209A mutant MHV-A59 virions. The data for diameters of plaques are means ± standard deviations (n = 50). All experiments were repeated at least three times.

cultures infected with H209A survived longer than cells infected with WT virus. Of note, the diameter of plaques formed by H209A virus in 17Cl.1 cells was only about 1/3 of that of WT virus (Fig. 5D), suggesting that the mutant virus spreads more slowly from cell to cell.

Since H209A virus produces more viruses after 24 h postinoculation even though its initial growth kinetics is significantly delayed, we then asked whether H209A virus could compete with WT virus during multiple-step growth kinetics and multiple rounds of passage. We mixed H209A viruses with WT viruses at a ratio of either 1 WT to 1 H209A (1:1) or 1 WT to 10 H209A (1:10) and then serially passaged each virus mixture

TABLE 1 Nucleotide sequencing analysis of residue 209 of S proteins from serially passaged viruses[a]

Passage	WT	WT:H209A (1:1)	WT:H209A (1:10)	H209A
P0	TTACCAA**CAT**GGTGG	TTACCAA**SMT**GGTGG	TTACCAA**GCT**GGTGG	TTACCAA**GCT**GGTGG
P1	TTACCAA**CAT**GGTGG	TTACCAA**CAT**GGTGG	TTACCAA**SMT**GGTGG	TTACCAA**GCT**GGTGG
P2	TTACCAA**CAT**GGTGG	TTACCAA**CAT**GGTGG	TTACCAA**CAT**GGTGG	TTACCAA**GCT**GGTGG
P3	TTACCAA**CAT**GGTGG	TTACCAA**CAT**GGTGG	TTACCAA**CAT**GGTGG	TTACCAA**GCT**GGTGG
P4	TTACCAA**CAT**GGTGG	TTACCAA**CAT**GGTGG	TTACCAA**CAT**GGTGG	TTACCAA**GCT**GGTGG
P5	TTACCAA**CAT**GGTGG	TTACCAA**CAT**GGTGG	TTACCAA**CAT**GGTGG	TTACCAA**GCT**GGTGG
P6	TTACCAA**CAT**GGTGG	TTACCAA**CAT**GGTGG	TTACCAA**CAT**GGTGG	TTACCAA**GCT**GGTGG
P7	TTACCAA**CAT**GGTGG	TTACCAA**CAT**GGTGG	TTACCAA**CAT**GGTGG	TTACCAA**GCT**GGTGG
P8	TTACCAA**CAT**GGTGG	TTACCAA**CAT**GGTGG	TTACCAA**CAT**GGTGG	TTACCAA**GCT**GGTGG
P9	TTACCAA**CAT**GGTGG	TTACCAA**CAT**GGTGG	TTACCAA**CAT**GGTGG	TTACCAA**GCT**GGTGG
P10	TTACCAA**CAT**GGTGG	TTACCAA**CAT**GGTGG	TTACCAA**CAT**GGTGG	TTACCAA**GCT**GGTGG

[a]Shown is the nucleotide sequence analysis of residue 209 of wild-type and mutant MHV-A59 S glycoproteins from cocultured viruses serially passaged in murine 17Cl.1 cells. S, C or G; M, A or C. The letters in bold represent the coding sequences for residue 209 of S proteins.

on murine 17Cl.1 cells at an MOI of 0.05 for 10 rounds. The nucleotide sequence at codon 209 was determined at each passage. As shown in Table 1 and data not shown, at the initial inoculation ratio of 1 WT to 1 H209A, WT virus outgrew H209A virus in a single passage. Even at the ratio of 1 WT to 10 H209A, WT virus outcompeted H209A virus after only two passages, indicating that WT virus has significant advantages over H209A virus in growth. As a control, we also passaged H209A virus for 10 rounds and detected no revertant mutation.

H209A mutation increased thermostability of MHV-A59 S protein. Mutant H209A S protein bound to the receptor as well as WT S protein, so why is H209A mutant MHV-A59 so attenuated? Recent analysis of Ebola viruses during the 2013-2016 outbreak (30, 31) found that mutation A82V in the viral glycoprotein (Gp) that arose during the pandemic may have contributed to the increasing rate of virus spread among humans. Later, Wang et al. (32) demonstrated that these A82V and T544I mutations in Ebolavirus Gp significantly decreased the stability of the glycoprotein while they increased virus infectivity in cell culture. We therefore investigated whether the H209A substitution had any effect on the stability of the MHV-A59 S protein and virus infectivity. Figure 6 shows that pseudovirions with the H209A mutant S protein were more stable than pseudovirions with WT S protein, requiring a significantly longer time (Fig. 6A) and higher temperature at pH 7.4 to be inactivated than the WT (Fig. 6B). Replacement of His 209 with Ala significantly increased the stability of the S protein, which likely increased the threshold for the receptor-induced and receptor-independent conformational changes of S protein that mediates membrane fusion and virus entry.

DISCUSSION

Entry of coronaviruses is a complicated process that has been the focus of many studies, although the detailed molecular mechanism remains elusive, including the effects of alkaline pH on receptor-independent entry and syncytium formation of MHV-A59. It has been over 27 years since Sturman et al. (18) first reported that incubation of MHV-A59 at pH 8.0 and 37°C without receptor caused conformational changes of S protein and reduced virus infectivity. Later, Zelus et al. (19) showed that the conformation changes of MHV-A59 S proteins triggered by pH 8.0 at 37°C without receptor were similar to those induced by receptor binding to S proteins at either pH 6.5 or pH 8.0. In this study, we also confirmed these results (Fig. 1). Moreover, we also found that pH 8.0 at 37°C can trigger WT MHV-A59 S protein to mediate receptor-independent syncytium formation on human 293T cells. To our knowledge, the S glycoprotein of MHV-A59 is the only viral glycoprotein for which either pH 8.0 alone or receptor binding at 37°C can trigger the conformational changes.

To determine how pH 8.0 at 37°C triggers the receptor-independent conformational change of WT MHV-A59 S protein, we mutated each individual histidine residue in the viral S protein to alanine and evaluated the contribution of each mutation to receptor-

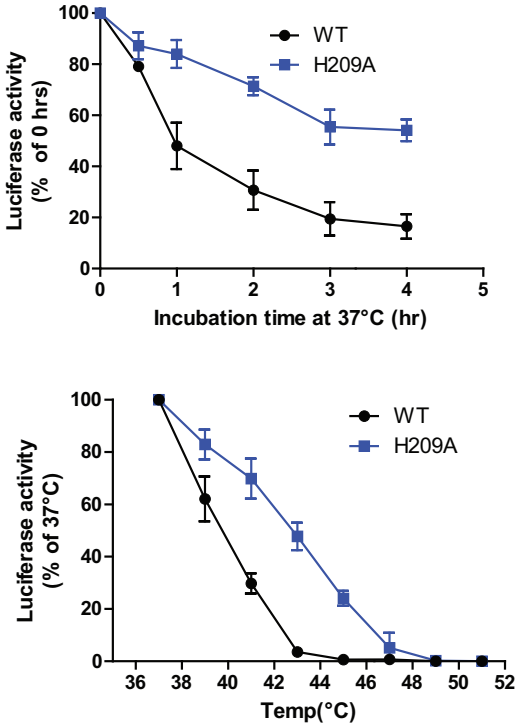

FIG 6 Stability of WT and H209A mutant MHV-A59 S proteins on lentivirus pseudovirions. (A) Lentiviruses pseudotyped with WT or H209A mutant S proteins were incubated at 37°C for the specified times (0 to 4 h) in the absence of serum, and then assayed on HeLa/mCEACAM1a cells. The results from infection at 0 h were set as 100%, and the experiments were repeated four times. (B) WT or H209A S protein pseudovirions without serum were incubated at the indicated temperature (37 to 51°C) for 1 h and then assayed on HeLa/mCEACAM1a cells. The results are reported as the percentage of transduction at 37°C. The experiments were repeated four times, and means with standard deviations are shown.

independent syncytium formation. We found that H179, H209, H441, H643, and H759 were critical for pH 8.0-triggered receptor-independent syncytium formation (Fig. 3A and B). While 8 of the 15 His residues in MHV-A59 S protein, including H179 and H643, are conserved in all of the MHV strains and H441 and H759 are also found in several of the other MHV strains, H209 is found only in the S protein of MHV-A59 (Fig. 7). In the structure of trimeric S proteins of MHV-A59 (33), all five residues, H179, H209, H441, H643, and H759, are accessible to the solvent. H179 is underneath the receptor-binding interface of the S1 subunit (Fig. 8); H209 is located inside the trimer but remains accessible to solvent; H441 is located on the top of the trimer and connects the insertion and the core subdomains of CTD of S protein; H643 is located at the end of β-sheet 20 of domain D and interacts with Y709; and H759 is located at the core

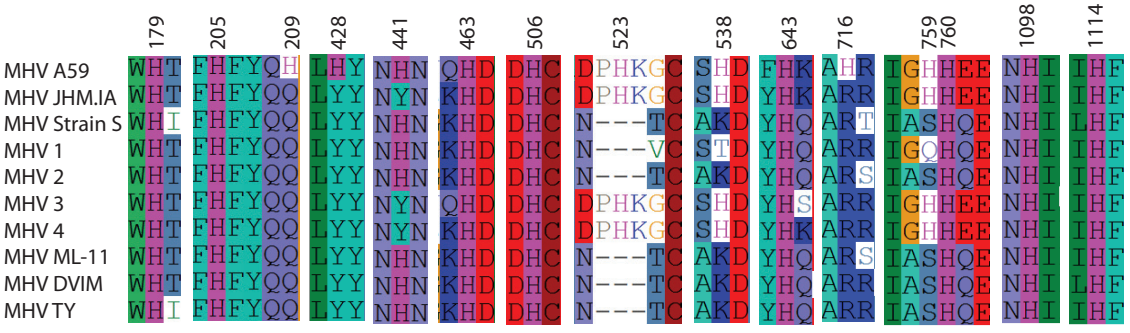

FIG 7 Alignment of amino acid sequences of S proteins of different MHV strains. The 15 His residues in MHV-A59 are shown in magenta. His209 is only found in MHV-A59. Amino acid numbers are derived from MHV-A59 S protein.

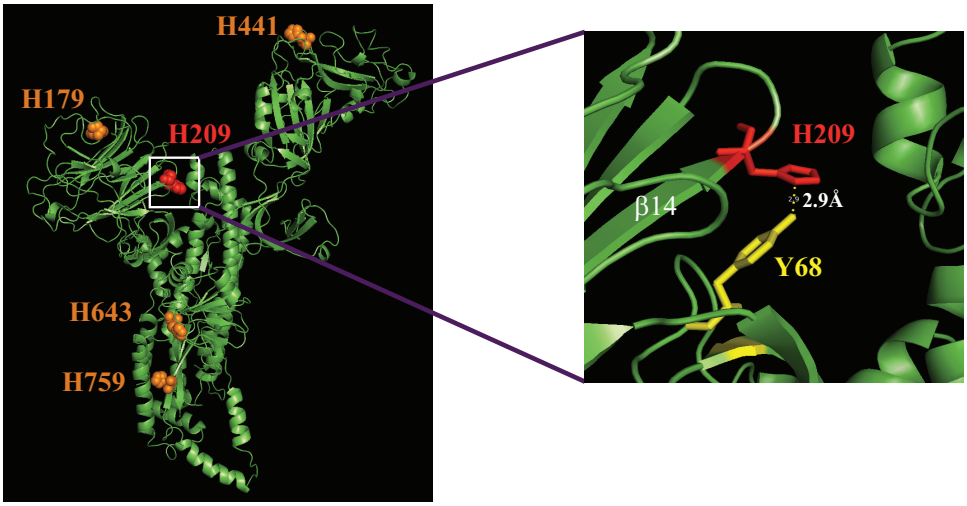

FIG 8 Ribbon structure of single monomer of the trimeric MHV-A59 S proteins. H179, H209, H441, H643, and H759 are shown in red spheres on the right and magnified structural details of the rectangular area on the left, showing that the imidazole ring of H209 interacts with Y68.

antiparallel β-sheet 46 of the S2 subunit and interacts with a nearby α-helix 27 on the same monomer (33). It is worth noting that among these five key histidine residues, only H209 seems to be essential for RIS, since replacement of His 209 with Ala almost completely abolished pH 8.0-induced RIS (Fig. 3). H209 only interacts with Y68 on β3 from the same monomer (Fig. 8). However, Y68F mutant showed WT levels of RIS when triggered by pH 8.0 (data not shown), suggesting that the interaction between Y68 and H209 is not essential for pH 8-triggered receptor-independent syncytium formation. Although the exact mechanism by which pH 8.0 triggers receptor-independent syncytium formation through H209 remains to be determined, it is possible that pH 8.0, which causes deprotonation of H209, alters the local conformation of β sheet 14, resulting in displacement of S1 from S2 and allowing the exposure of fusion peptide, insertion of fusion peptide into target membrane, formation of six-helix bundle formation, and ultimately membrane fusion.

During the 2013-2016 pandemic outbreak of the Ebolavirus in Africa, several new mutations, including A82V, on Ebolavirus Gp were identified that caused the increase of Ebolavirus infection of human cells and likely contributed to enhancement of transmission among humans (30, 31). Subsequently, Wang et al. (32) found that the A82V mutation did not affect virus binding but instead decreased the stability of the viral Gp, reducing the threshold for conformational changes of Gps that mediate membrane fusion and dependency for host entry factors, such as protease. Like Ebolavirus Gp, CoV S protein in its prefusion conformation is also metastable and can be triggered to undergo conformational changes by elevated temperature in the absence of receptor. Compared to the WT, the H209A mutant was stable at higher temperature and for a longer time before inactivation (Fig. 6), indicating that H209A substitution significantly stabilizes the native prefusion conformation of S protein. However, increased stability of S protein on virions by the H209A mutation apparently has a negative impact on its function. The H209A substitution reduced the S protein-mediated, receptor-dependent transduction by lentivirus pseudovirions by 30% (Fig. 4) compared to that of the WT, even though the H209A mutant S protein bound to the mCEACAM1a receptor as well as the WT did (Fig. 2). Moreover, the growth kinetics for the H209A mutant MHV-A59 virus in murine 17Cl.1 cells were significantly delayed, and its plaque diameter was much smaller than that of WT virus (Fig. 5). When mixed with WT virus, the H209A MHV-A59 virus, even at 10-fold excess, was easily outgrown by WT virus (Table 1), indicating that WT virus has much better fitness than H209A virus in this murine cell culture line. Similar phenomena also have been documented for the S

protein of MHV-JHM (34–36). Krueger et al. (34) previously reported that V870A and A1046V mutations in S2 of MHV JHM increased the association between S1 and S2 but decreased receptor-dependent syncytium formation; Ontiveros et al. (36) also found that S310G mutation in JHM.IA S protein increased virus virulence in mice at the cost of S protein stability. Of note, whether H209A mutant MHV-A59 virus is less fit or virulent, particularly neurovirulent, in mouse infection remains to be further determined.

The relationship between the stability of glycoproteins of other types of enveloped viruses and their fitness has been studied extensively (37–44). The pH stability of influenza virus hemagglutinin (HA) has been linked to differences in host adaptation and transmission. Whereas most isolates from pandemic H1N1 influenza from early 2009 infection had HAs that were relatively less thermostable and had higher pH thresholds for infection, the human isolates from more recently circulating pandemic H1N1 influenza viruses have evolved to increase their thermostability and lower their threshold pH for infectivity (37–40, 42). There is always a delicate balance between viral glycoprotein stability and fitness. The native prefusion viral envelope glycoprotein is metastable, and there is an energy barrier that prevents it from undergoing conformational change before triggering. Although glycoproteins with higher stability have a longer time to reach their next target cell in the harsh extracellular environment before losing their infectivity, the stable glycoproteins also potentially have a higher energy barrier for the conformational changes that leads to membrane fusion and reduced viral fitness. This is likely the case for our H209A mutant MHV-A59 virus.

In summary, using mutagenesis, we identified H209 as the essential residue responsible for higher pH-triggered and receptor-independent syncytium formation and showed that introduction of the H209A substitution raised thermal stability of the MHV-A59 viral S glycoprotein at the cost of viral fitness.

MATERIALS AND METHODS

Cell culture. Human HEK293T, 293/mCEACAM1a (293 cells stably expressing murine CEACAM1a), HeLa/mCEACAM1a (HeLa cells stably expressing murine CEACAM1a), murine 17Cl.1 (17Cl.1 line of BALB/c 3T3 fibroblasts), and *Felis catus* whole-fetus (FCWF) cells were maintained in Dulbecco's modified Eagle's medium (DMEM) (Invitrogen, Carlsbad, CA) supplemented with 10% fetal bovine serum (FBS) and 2% penicillin-streptomycin-amphotericin B (Invitrogen) at 37°C with 5% CO_2.

Constructs and mutagenesis. DNA encoding codon-optimized full-length MHV-A59 S protein was cloned between BamHI and NotI sites of pcDNA3.1 to generate pcDNA3-MHV S construct (15). All mutagenesis procedures were carried out using the Q5 mutagenesis kit (NEB, Ipswich, MA, USA). After the entire coding sequences were verified by sequencing, the BamHI- and NotI-containing mutated S gene was cloned back into pcDNA3-MHV-A59 S. To express soluble murine CEACAM1a (mCEACAM1a[1-4]), residues 1 to 236 of mCEACAM1a with 6His and AVI tags was cloned into EcoRI and NotI of pFASTBac1. The soluble receptor was expressed in High Five insect cells using the Bac-to-Bac system (Invitrogen) and purified through nickel affinity and ion-exchange chromatography (45).

Analysis of S protein expression on cell surface. Briefly, HEK293T cells were transfected with 2 μg of either wild-type or mutant S protein-expressing plasmid using polyethyleneimine (PEI) (Polysciences Inc., Warrington, PA, USA). Forty hours later, cells were detached from plates by incubating with phosphate-buffered saline (PBS) plus 1 mM EDTA for 5 min at 37°C. After washing, cells were incubated with goat polyclonal anti-MHV S antibody (AO4) (1:200 dilution), and then cells were stained with Alexa Fluor 488-conjugated rabbit anti-goat IgG (1:200) (ZSGB-Bio LLC, Beijing, China). Cells then were fixed with 1% paraformaldehyde and analyzed by flow cytometry.

Binding of soluble murine receptor. Human 293T cells were transfected with plasmids encoding either wild-type or mutant S proteins by PEI. After 40 h, cells were lifted with PBS plus 1 mM EDTA and immediately washed twice with PBS plus 2% normal donkey serum (NDS). About 2×10^5 cells were incubated with 10 μg of soluble mCEACAM1a[1-4] for 1 h on ice. After washing three times with PBS plus 2% NDS, cells were incubated with rabbit polyclonal anti-AVI antibody (1:200 dilution) (Shanghai Enzyme-Linked Biotechnology Co., Shanghai, China), followed by Alexa Fluor 488-conjugated goat anti-rabbit IgG (1:200). Cells were fixed with 1% paraformaldehyde and analyzed by flow cytometry.

Production and transduction of S protein-pseudotyped lentivirus. Lentivirus pseudovirions with MHV-A59 spike glycoproteins were produced as described previously, with minor modifications (46). Briefly, plasmid encoding either wild-type or mutant MHV-A59 S protein was cotransfected into 293T cells with pLenti-Luc-GFP (a gift from Fang Li, Duke University) and psPAX2 (Addgene, Cambridge, MA) at a molar ratio of 1:1:1 by using PEI. The next day, cells were fed with fresh medium at pH 6.5. After 24 h of incubation, the supernatant media containing pseudovirions were centrifuged at $800 \times g$ for 5 min to remove debris and passed through a 0.45-μm filter. To quantify MHV-A59 S protein-mediated entry of pseudovirions, susceptible cells were seeded at about 25 to 30% confluence in 24-well plates, and after

24 h the cells were inoculated with 500 μl of 1:1-diluted viruses. At 40 h postinoculation, cells were lysed at room temperature with 120 μl of medium with an equal volume of Steady-Glo (Promega, Madison, WI). Transduction efficiency was monitored by quantitation of luciferase activity using a Modulus II microplate reader (Turner Biosystems, Sunnyvale, CA). All experiments were done in triplicate and repeated at least three times.

Detection of viral spike glycoproteins by Western blotting. To evaluate S protein expression in cells, human 293T cells were transfected with plasmid encoding either wild-type or mutant MHV-A59 S proteins by using PEI. Forty hours later, cells were lysed with lysis buffer (50 mM Tris-HCl, pH 7.4, 150 mM NaCl, 2 mM EDTA, 1% Triton X-100, 0.1% SDS) with protease inhibitors (Roche). To determine S protein incorporation into pseudovirions, the virion-containing supernatant was pelleted through a 20% sucrose cushion at 30,000 rpm at 4°C for 2 h in a Beckman SW41 rotor (47). Viral pellets were resuspended in PBS. Cell lysate and pseudovirion pellet were separated on 4 to 15% SDS-PAGE and transferred to a nitrocellulose blot. The MHV-A59 S proteins were detected with polyclonal goat anti-MHV S antibody AO4 (1:2,000), and the blot was further stained with horseradish peroxidase-conjugated rabbit anti-goat IgG (1:10,000) and then visualized with Clarity Western ECL substrate (Bio-Rad, Hercules, CA, USA). The β-actin and HIV capsid protein (p24) were detected using mouse monoclonal anti-β-actin antibody (1:5,000) (Sigma, St. Louis, MO, USA) and rabbit polyclonal anti-p24 antibody (1:5,000) (Sinobiological Inc., Beijing, China).

Analysis of conformational changes of S proteins on pseudovirions by limited trypsin digestion. MHV-A59 S protein-pseudotyped lentiviruses were pelleted through a 20% sucrose in TMS buffer (25 mM Tris, 25 mM maleic acid, 150 mM NaCl, pH 6.5) at 30,000 rpm at 4°C for 2 h to remove serum. Virus pellets were resuspended in either TMS buffer at pH 6.5 or Tris-saline buffer (25 mM Tris, 150 mM NaCl, pH 8.0). Virus suspension was incubated alone or with 20 μg of soluble mCEACAM1a[1-4] for 30 min on ice to allow receptor binding and then shifted to either 4°C or 37°C for 30 min. After incubation, the virus-receptor mixture was quickly cooled down to 4°C. *N*-tosyl-L-phenylalanine chloromethyl ketone (TPCK)-treated trypsin was then added to each well to a final concentration of 20 μg/ml. After 30 min of incubation, a 5-fold excess of soybean trypsin inhibitor was added. Half of the samples were boiled with DTT and then separated by 4 to 15% SDS-PAGE; the other half, without DTT and boiling, were directly separated by 4 to 15% SDS-PAGE. After being transferred to a nitrocellulose blot, MHV-A59 S proteins were detected with polyclonal goat anti-MHV S antibody AO4 (1:2,000).

pH-triggered and receptor-independent cell-cell fusion assays. Human 293T cells were cotransfected with plasmids encoding MHV-A59 S glycoprotein and GFP using PEI. Twenty-four hours later, cells were fed with fresh medium at the indicated pH. After 3 h of incubation, and images (enhanced GFP [eGFP] and phase) of syncytia were captured with a Nikon TE2000 epifluorescence microscope running MetaMorph software (Molecular Devices). For each mutant, four to six randomly selected images were chosen, and for each image, the total number of nuclei in syncytia (eGFP image) and the total number of cells (phase image; 600 to 800 cells/image) were counted and percentage of nuclei in syncytia was calculated as the total number of nuclei in syncytia/number of total cells $\times$ 100. To quantify the cell-cell fusion, 293T cells were transfected with pBE-NF-κB. The next day, the cells were lifted with trypsin and overlaid onto 293T cells cotransfected with pFR-Luc and plasmid encoding MHV-A59 S protein at a ratio of about one to one at the indicated pH. After 6 h of incubation, cells were lysed by adding 120 μl of media with an equal volume of Steady-Glo and medium, and luciferase activity was measured with a Modulus II microplate reader. All experiments were done in triplicate and repeated at least three times.

TRR. Targeted RNA recombination (TRR) was carried out as described previously, with minor modifications (48–50). Briefly, individual mutations were introduced into the pMH54 plasmid using the Q5 mutagenesis kit. After sequences were verified, DNA fragments containing each desired mutation were cloned back into the pMH54 plasmid between the AvrII and SbfI sites. Capped transcripts were synthesized from a PacI-linearized pMH54 construct *in vitro* using an mMessage mMachine T7 kit (Ambion, Austin, TX, USA) and transfected into feline MHV-inoculated FCWF cells using a Neon transfection system (ThermoFisher Scientific, Waltham, MA, USA). The transfected FCWF cells were immediately overlaid on murine 17Cl.1 cells. After 48 h of incubation, virus-containing supernatant was harvested and centrifuged to remove cell debris and then flash frozen at −80°C.

Growth competition of WT and mutant MHV-A59 viruses. WT and mutant MHV-A59 viruses were mixed at different ratios, and the mixed viruses were inoculated onto murine 17Cl.1 cells at an MOI of 0.05. One hour later, inocula were removed and replaced with fresh medium. After another 23 h of incubation, virus-containing supernatants were harvested and centrifuged to remove cell debris. Virus titers were determined by plaque assay, and virus was again inoculated at an MOI of 0.05 and propagated on 17Cl.1 cells. The whole process was repeated 10 times, the viral RNAs from each round were extracted and amplified by reverse transcription-PCR, and S genes were sequenced.

Virus thermal inactivation. WT or mutant MHV-A59 S protein-pseudotyped lentiviruses were pelleted through 20% sucrose in TMS buffer by centrifugation at 30,000 rpm at 4°C for 2 h in a Beckman SW41 rotor. Viruses were resuspended in DMEM (pH 7.4) without serum and incubated either at the specified temperature (37 to 51°C) for 1 h or at 37°C for the specified time (0 to 4 h). After cooling to room temperature, viruses were inoculated onto HeLa/mCEACAM1a cells to assay their remaining transduction capability.

ACKNOWLEDGMENTS

This work was supported by grants from Chinese Science and Technology Key Projects (2016YFC1200200-002), the National Natural Science Foundation of China (31670164, 31470266, and 81702013), the CAMS Innovation Fund for Medical Sciences

(2016-12M-1-014), the CAMS general fund (2016ZX310052), and the PUMC Youth Fund and the Fundamental Research Funds for the Central Universities (2017310020).

REFERENCES

1. White J, Matlin K, Helenius A. 1981. Cell fusion by Semliki Forest, influenza, and vesicular stomatitis viruses. J Cell Biol 89:674–679. https://doi.org/10.1083/jcb.89.3.674.
2. White JM, Delos SE, Brecher M, Schornberg K. 2008. Structures and mechanisms of viral membrane fusion proteins: multiple variations on a common theme. Crit Rev Biochem Mol Biol 43:189–219. https://doi.org/10.1080/10409230802058320.
3. Srinivasakumar N, Ogra PL, Flanagan TD. 1991. Characteristics of fusion of respiratory syncytial virus with HEp-2 cells as measured by R18 fluorescence dequenching assay. J Virol 65:4063–4069.
4. Stein BS, Gowda SD, Lifson JD, Penhallow RC, Bensch KG, Engleman EG. 1987. pH-independent HIV entry into CD4-positive T cells via virus envelope fusion to the plasma membrane. Cell 49:659–668. https://doi.org/10.1016/0092-8674(87)90542-3.
5. Masters PS, Perlman S. 2013. Coronaviridae, p 825–858. *In* Knipe DM, Howley PM, Cohen JI, Griffin DE, Lamb RA, Martin MA, Racaniello VR, Roizman B (ed), Fields virology, 6th ed, vol 1. Lippincott Williams & Wilkins, Philadelphia, PA.
6. International Committee on Taxonomy of Viruses. 2011. Virus taxonomy: 2011 release. Elsevier Academic Press, San Diego, CA. http://ictvonline.org/virusTaxonomy.asp?version=2011.
7. Williams RK, Jiang GS, Holmes KV. 1991. Receptor for mouse hepatitis virus is a member of the carcinoembryonic antigen family of glycoproteins. Proc Natl Acad Sci U S A 88:5533–5536. https://doi.org/10.1073/pnas.88.13.5533.
8. Bosch BJ, van der Zee R, de Haan CA, Rottier PJ. 2003. The coronavirus spike protein is a class I virus fusion protein: structural and functional characterization of the fusion core complex. J Virol 77:8801–8811. https://doi.org/10.1128/JVI.77.16.8801-8811.2003.
9. de Haan CA, Stadler K, Godeke GJ, Bosch BJ, Rottier PJ. 2004. Cleavage inhibition of the murine coronavirus spike protein by a furin-like enzyme affects cell-cell but not virus-cell fusion. J Virol 78:6048–6054. https://doi.org/10.1128/JVI.78.11.6048-6054.2004.
10. Peng G, Sun D, Rajashankar KR, Qian Z, Holmes KV, Li F. 2011. Crystal structure of mouse coronavirus receptor-binding domain complexed with its murine receptor. Proc Natl Acad Sci U S A 108:10696–10701. https://doi.org/10.1073/pnas.1104306108.
11. Kubo H, Yamada YK, Taguchi F. 1994. Localization of neutralizing epitopes and the receptor-binding site within the amino-terminal 330 amino acids of the murine coronavirus spike protein. J Virol 68:5403–5410.
12. Wicht O, Burkard C, de Haan CA, van Kuppeveld FJ, Rottier PJ, Bosch BJ. 2014. Identification and characterization of a proteolytically primed form of the murine coronavirus spike proteins after fusion with the target cell. J Virol 88:4943–4952. https://doi.org/10.1128/JVI.03451-13.
13. Belouzard S, Chu VC, Whittaker GR. 2009. Activation of the SARS coronavirus spike protein via sequential proteolytic cleavage at two distinct sites. Proc Natl Acad Sci U S A 106:5871–5876. https://doi.org/10.1073/pnas.0809524106.
14. Park JE, Li K, Barlan A, Fehr AR, Perlman S, McCray PB, Jr, Gallagher T. 2016. Proteolytic processing of Middle East respiratory syndrome coronavirus spikes expands virus tropism. Proc Natl Acad Sci U S A 113:12262–12267. https://doi.org/10.1073/pnas.1608147113.
15. Ou X, Zheng W, Shan Y, Mu Z, Dominguez SR, Holmes KV, Qian Z. 2016. Identification of the fusion peptide-containing region in betacoronavirus spike glycoproteins. J Virol 90:5586–5600. https://doi.org/10.1128/JVI.00015-16.
16. Phillips JM, Gallagher T, Weiss SR. 1 February 2017. Neurovirulent murine coronavirus JHM.SD uses cellular zinc metalloproteases for virus entry and cell-cell fusion. J Virol https://doi.org/10.1128/JVI.01564-16.
17. Qiu Z, Hingley ST, Simmons G, Yu C, Das Sarma J, Bates P, Weiss SR. 2006. Endosomal proteolysis by cathepsins is necessary for murine coronavirus mouse hepatitis virus type 2 spike-mediated entry. J Virol 80:5768–5776. https://doi.org/10.1128/JVI.00442-06.
18. Sturman LS, Ricard CS, Holmes KV. 1990. Conformational change of the coronavirus peplomer glycoprotein at pH 8.0 and 37 degrees C correlates with virus aggregation and virus-induced cell fusion. J Virol 64:3042–3050.
19. Zelus BD, Schickli JH, Blau DM, Weiss SR, Holmes KV. 2003. Conformational changes in the spike glycoprotein of murine coronavirus are induced at 37°C either by soluble murine CEACAM1 receptors or by pH 8. J Virol 77:830–840. https://doi.org/10.1128/JVI.77.2.830-840.2003.
20. Pu Y, Zhang X. 2008. Mouse hepatitis virus type 2 enters cells through a clathrin-mediated endocytic pathway independent of Eps15. J Virol 82:8112–8123. https://doi.org/10.1128/JVI.00837-08.
21. Eifart P, Ludwig K, Bottcher C, de Haan CA, Rottier PJ, Korte T, Herrmann A. 2007. Role of endocytosis and low pH in murine hepatitis virus strain A59 cell entry. J Virol 81:10758–10768. https://doi.org/10.1128/JVI.00725-07.
22. Burkard C, Verheije MH, Wicht O, van Kasteren SI, van Kuppeveld FJ, Haagmans BL, Pelkmans L, Rottier PJ, Bosch BJ, de Haan CA. 2014. Coronavirus cell entry occurs through the endo-/lysosomal pathway in a proteolysis-dependent manner. PLoS Pathog 10:e1004502. https://doi.org/10.1371/journal.ppat.1004502.
23. Walls AC, Tortorici MA, Snijder J, Xiong X, Bosch BJ, Rey FA, Veesler D. 2017. Tectonic conformational changes of a coronavirus spike glycoprotein promote membrane fusion. Proc Natl Acad Sci U S A 114:11157–11162. https://doi.org/10.1073/pnas.1708727114.
24. Nelson DL, Cox MM. 2012. Lehninger principles of biochemistry, 6th ed. W. H. Freeman & Co, New York, NY.
25. Bressanelli S, Stiasny K, Allison SL, Stura EA, Duquerroy S, Lescar J, Heinz FX, Rey FA. 2004. Structure of a flavivirus envelope glycoprotein in its low-pH-induced membrane fusion conformation. EMBO J 23:728–738. https://doi.org/10.1038/sj.emboj.7600064.
26. Carneiro FA, Stauffer F, Lima CS, Juliano MA, Juliano L, Da Poian AT. 2003. Membrane fusion induced by vesicular stomatitis virus depends on histidine protonation. J Biol Chem 278:13789–13794. https://doi.org/10.1074/jbc.M210615200.
27. Mair CM, Meyer T, Schneider K, Huang Q, Veit M, Herrmann A. 2014. A histidine residue of the influenza virus hemagglutinin controls the pH dependence of the conformational change mediating membrane fusion. J Virol 88:13189–13200. https://doi.org/10.1128/JVI.01704-14.
28. Kampmann T, Mueller DS, Mark AE, Young PR, Kobe B. 2006. The role of histidine residues in low-pH-mediated viral membrane fusion. Structure 14:1481–1487. https://doi.org/10.1016/j.str.2006.07.011.
29. Gallagher TM, Escarmis C, Buchmeier MJ. 1991. Alteration of the pH dependence of coronavirus-induced cell fusion: effect of mutations in the spike glycoprotein. J Virol 65:1916–1928.
30. Diehl WE, Lin AE, Grubaugh ND, Carvalho LM, Kim K, Kyawe PP, McCauley SM, Donnard E, Kucukural A, McDonel P, Schaffner SF, Garber M, Rambaut A, Andersen KG, Sabeti PC, Luban J. 2016. Ebola virus glycoprotein with increased infectivity dominated the 2013–2016 epidemic. Cell 167:1088–1098.
31. Urbanowicz RA, McClure CP, Sakuntabhai A, Sall AA, Kobinger G, Muller MA, Holmes EC, Rey FA, Simon-Loriere E, Ball JK. 2016. Human adaptation of Ebola virus during the West African outbreak. Cell 167:1079–1087. https://doi.org/10.1016/j.cell.2016.10.013.
32. Wang MK, Lim SY, Lee SM, Cunningham JM. 2017. Biochemical basis for increased activity of Ebola glycoprotein in the 2013-16 epidemic. Cell Host Microbe 21:367–375. https://doi.org/10.1016/j.chom.2017.02.002.
33. Walls AC, Tortorici MA, Bosch BJ, Frenz B, Rottier PJ, DiMaio F, Rey FA, Veesler D. 2016. Cryo-electron microscopy structure of a coronavirus spike glycoprotein trimer. Nature 531:114–117. https://doi.org/10.1038/nature16988.
34. Krueger DK, Kelly SM, Lewicki DN, Ruffolo R, Gallagher TM. 2001. Variations in disparate regions of the murine coronavirus spike protein impact the initiation of membrane fusion. J Virol 75:2792–2802. https://doi.org/10.1128/JVI.75.6.2792-2802.2001.
35. Matsuyama S, Taguchi F. 2002. Communication between S1N330 and a region in S2 of murine coronavirus spike protein is important for virus entry into cells expressing CEACAM1b receptor. Virology 295:160–171. https://doi.org/10.1006/viro.2002.1391.
36. Ontiveros E, Kim TS, Gallagher TM, Perlman S. 2003. Enhanced virulence

mediated by the murine coronavirus, mouse hepatitis virus strain JHM, is associated with a glycine at residue 310 of the spike glycoprotein. J Virol 77:10260–10269. https://doi.org/10.1128/JVI.77.19.10260-10269.2003.
37. Ambrose CS, Bright H, Mallory R. 2016. Letter to the editor: potential causes of the decreased effectiveness of the influenza A(H1N1)pdm09 strain in live attenuated influenza vaccines. Euro Surveill 21:30394. https://doi.org/10.2807/1560-7917.ES.2016.21.45.30394.
38. Cotter CR, Jin H, Chen Z. 2014. A single amino acid in the stalk region of the H1N1pdm influenza virus HA protein affects viral fusion, stability and infectivity. PLoS Pathog 10:e1003831. https://doi.org/10.1371/journal.ppat.1003831.
39. Di Lella S, Herrmann A, Mair CM. 2016. Modulation of the pH stability of influenza virus hemagglutinin: a host cell adaptation strategy. Biophys J 110:2293–2301. https://doi.org/10.1016/j.bpj.2016.04.035.
40. Farnsworth A, Cyr TD, Li C, Wang J, Li X. 2011. Antigenic stability of H1N1 pandemic vaccines correlates with vaccine strain. Vaccine 29:1529–1533. https://doi.org/10.1016/j.vaccine.2010.12.120.
41. Dessau M, Goldhill D, McBride R, Turner PE, Modis Y. 2012. Selective pressure causes an RNA virus to trade reproductive fitness for increased structural and thermal stability of a viral enzyme. PLoS Genet 8:e1003102. https://doi.org/10.1371/journal.pgen.1003102.
42. Mair CM, Ludwig K, Herrmann A, Sieben C. 2014. Receptor binding and pH stability–how influenza A virus hemagglutinin affects host-specific virus infection. Biochim Biophys Acta 1838:1153–1168. https://doi.org/10.1016/j.bbamem.2013.10.004.
43. Presloid JB, Mohammad TF, Lauring AS, Novella IS. 2016. Antigenic diversification is correlated with increased thermostability in a mammalian virus. Virology 496:203–214. https://doi.org/10.1016/j.virol.2016.06.009.
44. Wasik BR, Bhushan A, Ogbunugafor CB, Turner PE. 2015. Delayed transmission selects for increased survival of vesicular stomatitis virus. Evolution 69:117–125. https://doi.org/10.1111/evo.12544.
45. Ou X, Guan H, Qin B, Mu Z, Wojdyla JA, Wang M, Dominguez SR, Qian Z, Cui S. 2017. Crystal structure of the receptor binding domain of the spike glycoprotein of human betacoronavirus HKU1. Nat Commun 8:15216. https://doi.org/10.1038/ncomms15216.
46. Qian Z, Dominguez SR, Holmes KV. 2013. Role of the spike glycoprotein of human Middle East respiratory syndrome coronavirus (MERS-CoV) in virus entry and syncytia formation. PLoS One 8:e76469. https://doi.org/10.1371/journal.pone.0076469.
47. Qian Z, Wang H, Empig C, Anderson WF, Albritton LM. 2004. Complementation of a binding-defective retrovirus by a host cell receptor mutant. J Virol 78:5766–5772. https://doi.org/10.1128/JVI.78.11.5766-5772.2004.
48. Masters PS, Koetzner CA, Kerr CA, Heo Y. 1994. Optimization of targeted RNA recombination and mapping of a novel nucleocapsid gene mutation in the coronavirus mouse hepatitis virus. J Virol 68:328–337.
49. Thackray LB, Turner BC, Holmes KV. 2005. Substitutions of conserved amino acids in the receptor-binding domain of the spike glycoprotein affect utilization of murine CEACAM1a by the murine coronavirus MHV-A59. Virology 334:98–110. https://doi.org/10.1016/j.virol.2005.01.016.
50. Kuo L, Godeke GJ, Raamsman MJ, Masters PS, Rottier PJ. 2000. Retargeting of coronavirus by substitution of the spike glycoprotein ectodomain: crossing the host cell species barrier. J Virol 74:1393–1406. https://doi.org/10.1128/JVI.74.3.1393-1406.2000.